ISSN 1810-2328, Journal of Engineering Thermophysics, 2021, Vol. 30, No. 2, pp. 317–323. © Pleiades Publishing, Ltd., 2021.

Features of Setting Boundary Conditions in Problems of Modeling Turbulent Gas Motion in Turning-and-Expanding Flow for k-ε Turbulence Model and Reynolds Stress Transfer Model

I. K. Kabardin[1*], V. V. Kolotilov[2], E. V. Usov[2], N. I. Yavorsky[1*], A. K. Kabardin[1], S. V. Kakaulin[1], M. R. Gordienko[1], V. I. Polyakova[1], M. Kh. Pravdina[1], and O. G. Derzho[1]

[1]*Kutateladze Institute of Thermophysics, Siberian Branch, Russian Academy of Sciences, Novosibirsk, Russia*

[2]*Nuclear Safety Institute, Novosibirsk Branch, Russian Academy of Sciences, Novosibirsk, Russia*

Received April 7, 2021; in final form, April 26, 2021; accepted April 30, 2021

Abstract—The paper substantiates selection of boundary conditions for correct modeling of gas motion in a turning-and-expanding flow. The choice is based on comparison of calculation results and experimental data. Measurements of average and pulsation values of flow velocity were carried out by the method of laser Doppler anemometry. The numerical modelling was performed on the basis of known modern turbulence models: k-ε model and Reynolds stress transfer model. A comparative analysis of the models was done. The comparison was made for the surfaces of the axial velocity component in a cross section. The data obtained can be useful for determination of the limits of applicability of various turbulence models and for verifying CFD codes.

DOI: 10.1134/S1810232821020120

INTRODUCTION

The fundamental scientific problem of control of turning-and-diverging flow for optimization of the mass transfer arises in mechanics, chemistry, and catalysis. The efficiency of the mass transfer depends on the uniformity of the velocity fields and small-scale turbulence in the reacting flow [1]. Flows of reagents in real installations and reactors take place in complex geometry conditions with turning and expanding sections, in which flow separation occurs and near-wall jets and reverse flow zones arise. Such effects, as a rule, increase the hydrodynamic resistance of flow and deteriorate the uniformity of the turbulent mass transfer. Numerical modeling of such phenomena requires verification and modernization of turbulence models for adequate description of the mass transfer. The present work continues work [2], where experimental studies on control of turning-and-diverging flow with detailed diagnostics of averaged and turbulent characteristics were carried out. In work [2], numerical modeling and comparison with experimental data were performed on the basis of well-known modern turbulence models, and a comparative analysis of the models was done. It has been shown that the gas motion in a turning-and-diverging cross section is best described via calculations based on the application of the k-ε turbulence model [3] and the Reynolds stress transfer model [4]. However, comparison of the calculation results and experimental data has revealed that the discrepancy between the experiment and calculations is very different and achievement of adequate results necessitates more accurate setting of boundary conditions.

The objective of the work was to justify choice of most appropriate inlet boundary conditions for better modeling of gas flow in turning-and-expanding devices. The choice of boundary conditions was done on the basis of comparison of calculation results and experimental data.

*E-mail: ivankabardin@gmail.com

BRIEF DESCRIPTION OF EXPERIMENTAL STAND

For determination of the scope of applicability of turbulence models to the problems of enhancement of heat and mass transfer in a turning-and-diverging flow, a working section (Fig. 1) [1,2] and an aerodynamic measuring stand for testing it (Fig. 2) were created. The air was supplied to the working section through a fan; then the gas flow passed through a flow meter. The temperature in the flow was measured by a temperature sensor and the excess pressure, by excess pressure sensors. The hydraulic resistance of the flow was determined from the differential pressure on a rotator and the section before another rotator, measured by differential pressure sensors.

The overall dimensions of the working section were 600 × 3000 × 2300 mm. The ratio of the outlet area to the inlet area was 5 to 1. The shape of the outlet cross section after the first turn was a rectangle whose aspect ratio was 2 : 3. The flow turn angle was 90°. The working medium was air. The static

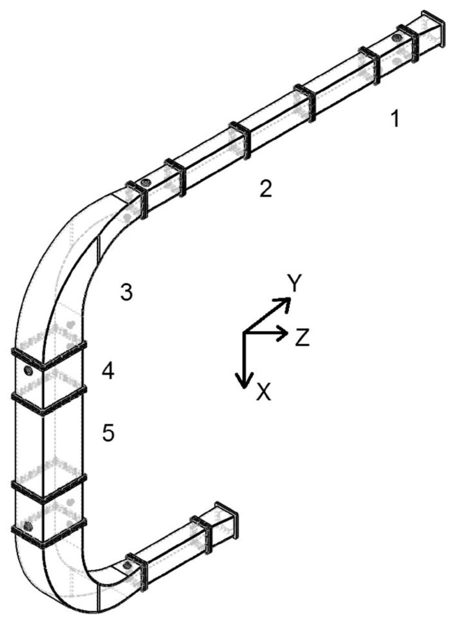

Fig. 1. 3D model of working section (1—inlet; 2—section before rotator, 3—rotator, 4—control section, 5—section before second rotator).

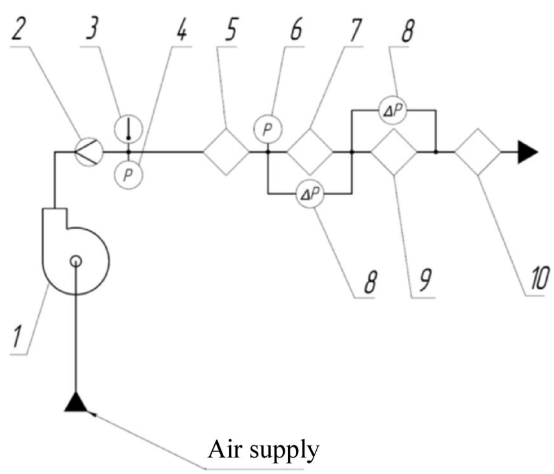

Fig. 2. Structural chart of stand: 1—fan, 2—flow meter, 3—temperature sensor, 4 and 6—overpressure converter, 5—area before turn, 8—differential pressure converter, 9—mixer, 7 and 10—rotary section.

pressure limit was 150 kPa. The inlet flow temperature was +10 . . . + 35°C. The mass flow rate was equal to 250 nm^3/h.

The aerodynamic stand contained an instrumentation system for measurement and registration of parameters, the information displayed on the computer screen. Data registration from sensors and control of the breadboard were carried out using a programmable logic controller.

The flow motion in the turning-diverging device was studied experimentally using the laser Doppler anemometry method [2]. A smoke generator seeded the flow with tracers. Portions of the generated smoke entered the 20 l container, and then the external pressure delivered the smoke to the fan and then to the pipe. Thus, the flow inside the experimental stand was seeded with tracer particles uniformly in time, which enabled measurement of the flow by the LDA method. 4000 measurements were made at each point. For adequate measurement of the surfaces of the axial velocity component, the mesh of coordinates of measurement points was made uneven. Near the wall, at a distance of 0 to 1.5 mm, the mesh step was 0.1 mm; at a distance from the wall of 1.5 mm to 3 mm, the mesh step was 0.5 mm; at a distance of 3.5 to 7.5 mm, the mesh step was 2 mm; in the flow core, the mesh step was 10 mm.

So, data on the velocity distribution were obtained and the structure of gas flows and the degree of gas flow inhomogeneity were analyzed. The measurements were carried out in three cross sections (Fig. 3): at the entrance to the breadboard, in the cross section before the first turn, and in the measurement

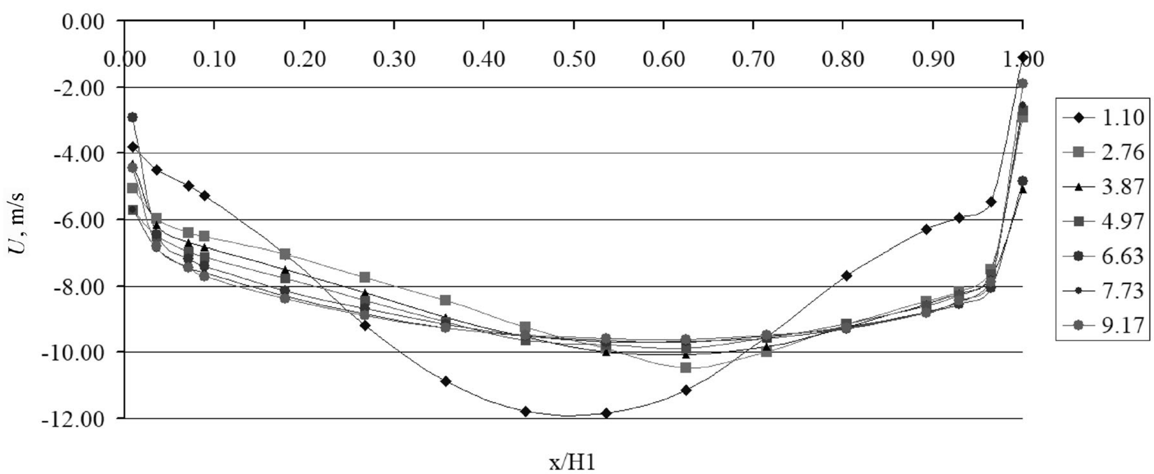

Fig. 3. Profiles of axial velocity component in median plane at different distances from inlet section. Steady profile was achieved at relative distance of y1=y/D1=6.63, where D1 = 96 mm is the hydraulic diameter at the inlet.

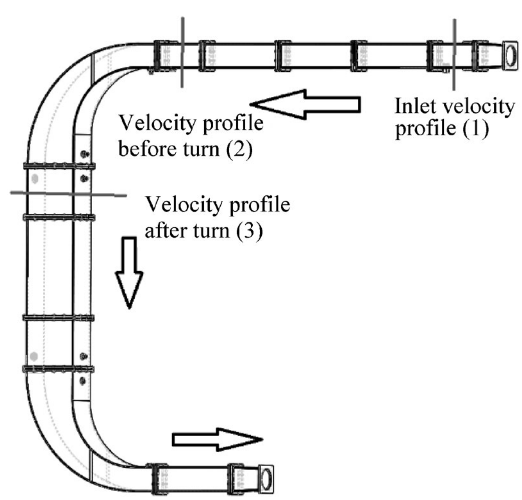

Fig. 4. Chart of velocity profile measurement.

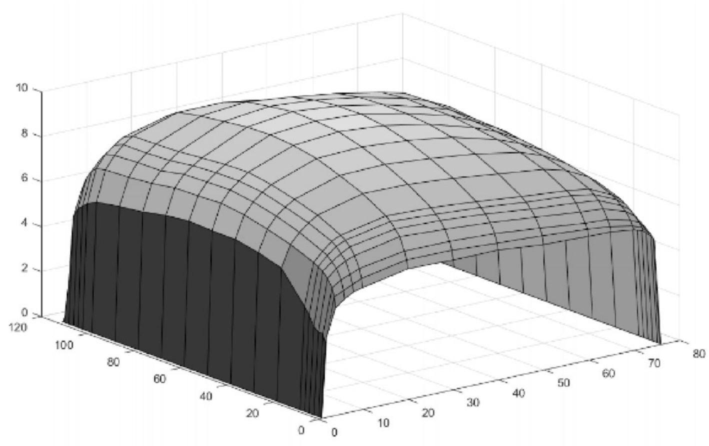

Fig. 5. Distribution of axial velocity component in section 1, measured at mass flow rate of 250 nm^3/h.

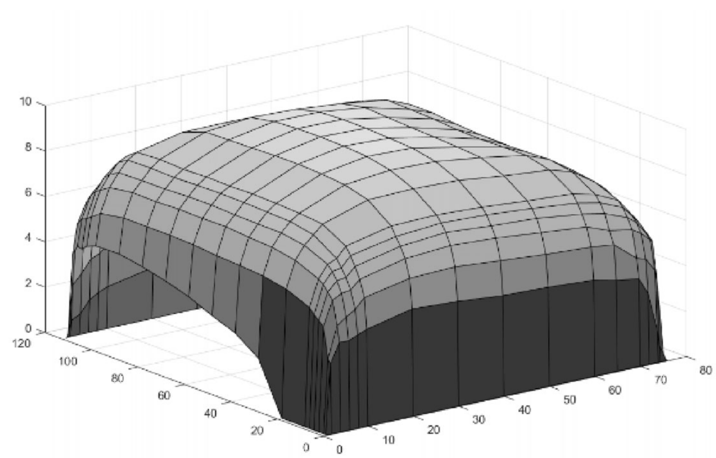

Fig. 6. Distribution of axial velocity component in cross section 2 at mass flow rate of 250 nm^3/h.

section before the catalyst cartridge after the first turn. First, the distance from the inlet was chosen at which the field of the axial velocity component settled (see Fig. 3). The steady profile was achieved at the relative distance $y/D1 = 6.63$ from the inlet.

Figures 4 and 5 present the results of measurement of the velocity profiles for cross sections 1 and 2. The pattern of the flow structure shows that the velocity profile in section 1 had settled, and it can be used for setting of the boundary and initial conditions.

Figures 6 and 7 show the flow structure after the turning section of the model. The measurement results demonstrate that the velocity profile was uneven. The formation of a powerful wall jet and a zone of return flow was observed. A recirculation zone appeared due to the sharp turn of the flow.

METHODS OF MATHEMATICAL MODELING

A detailed description of the calculation method is presented in [2]. Two turbulence models are used in this work: the k-ε and Reynolds stress transfer models, each having advantages and disadvantages. The k-ε turbulence model shows good results for many engineering applications, has high reliability and low computational costs, and is simple to use. But this model is limited by the assumption about the value of the turbulent viscosity and does not take into account the convection and diffusion of tangential stresses. The Reynolds stress transfer model can be applied to a complex flow, where turbulent viscosity models do not work. The Reynolds stress transfer model takes into account the flow anisotropy and describes well complicated flows, e.g., those with high vorticity, flow separation, and formation of jets. At the same time, the Reynolds stress transfer model requires large computational resources.

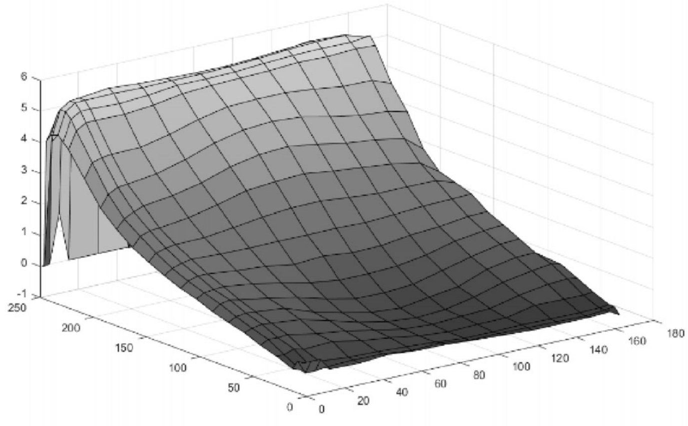

Fig. 7. Distribution of axial velocity component in cross section 3 at mass flow rate of 250 nm^3/h.

The numerical modeling of turbulent gas flow was based on solving the system of continuity equations, Navier–Stokes equations [2]. The medium was considered to be incompressible and isothermal. To close the averaged equations, two turbulence models were used: the k-ε model [3] and the Reynolds stress transfer model [4]. More information on the numerical modeling can also be found in [4].

For the k-ε model, the boundary conditions on a solid surface are formulated as follows. The velocity component normal to the surface is equal to zero. For the tangential component of the velocity, the slip condition is used. The inlet conditions were set for cross section 1, and thus approximations under these conditions did not affect the modeling results. For a better approximation, the turbulence intensity and turbulence length scale were used. The turbulence intensity was estimated experimentally. The characteristic scale was defined as $l = 0.07$ L, where L = 0.092 m is the hydraulic diameter and U = 12.2 m/s is the average flow rate. The values k and ε are estimated from the following formulas [4]:

$$k = \frac{3}{2}\left(\langle U\rangle\right)^2 \ \text{ and } \ \varepsilon = C_\mu^{3/4}\frac{k^{3/2}}{l}. \tag{1}$$

Setting the boundary conditions for the Reynolds stress transfer model is more difficult because of the necessity to specify all stresses. The initial conditions were set as follows. A correct initial state was estimated in several iterations. In the first step, calculations were performed with inlet-set experimental profiles of the kinetic energy of the turbulence and axial velocity components. After that, the Reynolds stresses calculated at some distance from cross section 1 were set on the inlet to cross section 1 and calculations were performed. The iterations were repeated until the difference between the calculated values of the Reynolds stresses was less than a required error value.

MODELING RESULTS

A three-dimensional model of the test bench was prepared for the mathematical modeling. The parameters of the model fully corresponded to the parameters of the test bench. The mathematical model contained 1,500,000 computational cells.

An uneven mesh was used (Fig. 8). Near the wall, the mesh was rectangular. The radial cell size varied from 0.1 to 0.2 mm. In the flow core, the mesh was triangular with a size of about 8 mm.

Figures 8–11 compare the results of the experiments, measurement, and modeling. Each figure shows the experimental surfaces of the axial velocity component in the cross section $U(\mathrm{x}, \mathrm{y})$, as well as the experimental surfaces of the axial velocity component, which reflect the limits of measurement errors $U(\mathrm{x}, \mathrm{y}) - \delta U(\mathrm{x}, \mathrm{y})$ and $U(\mathrm{x}, \mathrm{y}) + \delta U(\mathrm{x}, \mathrm{y})$, as well as the surface of the axial velocity component obtained from the calculations. From Figs. 8 and 9 it can be seen that in cross section 2, the surfaces of the axial velocity component calculated by both turbulence models lie between the surfaces reflecting the error boundaries. From cross section 3 in Figs. 10 and 11, one can see that the field of the axial velocity component calculated by the k-ε turbulence model goes slightly beyond the error boundaries, whereas the Reynolds stress transfer model falls within the error.

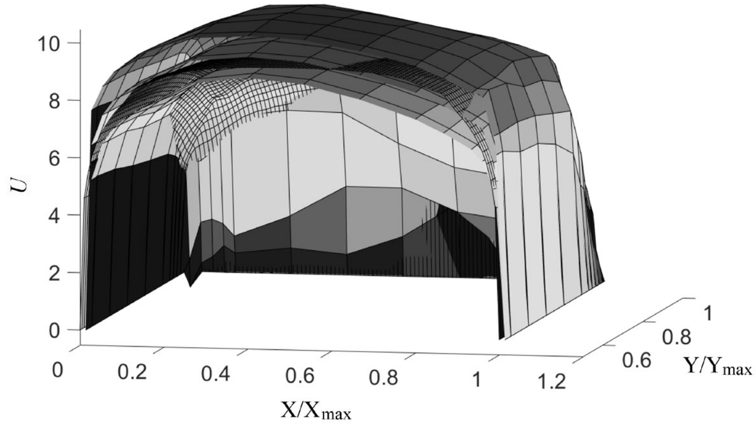

Fig. 8. Comparison of results of experiment, measurement, and modeling for cross section 2. Experimental surfaces of axial velocity component, which reflect limits of measurement errors, are shown, as well as surface of axial velocity component obtained from calculations using k-ε turbulence model.

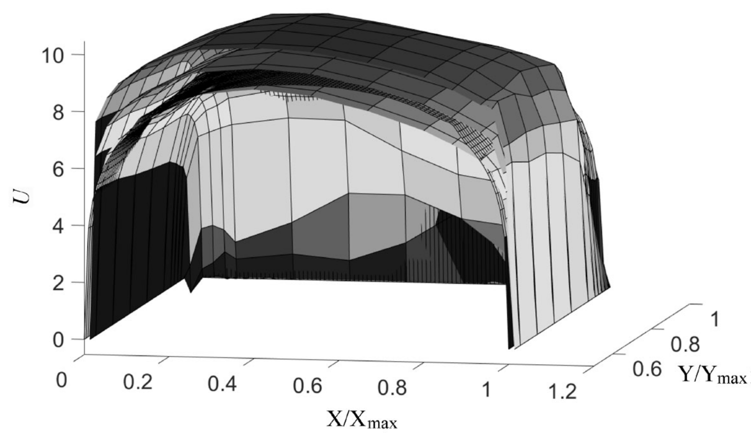

Fig. 9. Comparison of results of experiment, measurement, and modeling for cross section 2. Experimental surfaces of axial velocity component, which reflect limits of measurement errors, are shown, as well as surface of axial velocity component obtained from calculations using Reynolds stress transfer model.

CONCLUSIONS

An experimental stand was created for studying the characteristics of turbulent mass transfer. The laser Doppler anemometry method was used for the study of turbulent flows. A mathematical model was developed, on the basis of which a turning-and-diverging turbulent flow was modeled. Different semi-empirical turbulence models were used to close the averaged equations. It has been shown that correct setting of boundary conditions is essential for correct calculation of flow. Comparison of the results of the experiments, measurement, and modeling for several cross sections with respect to the experimental surfaces of the axial velocity component, which reflect the measurement error boundaries, has been carried out. It has been shown that the Reynolds stress transfer model better describes the flow.

FUNDING

The study of flow was carried out within the framework of the state assignment of the IT SB RAS (project 121032200034-4). The development of the software and hardware complex was performed within grant MD-1767.2020.8. The Doppler anemometry method was developed within the framework of IT SO RAN state assignment project (AAA-A19-119052190039-8).

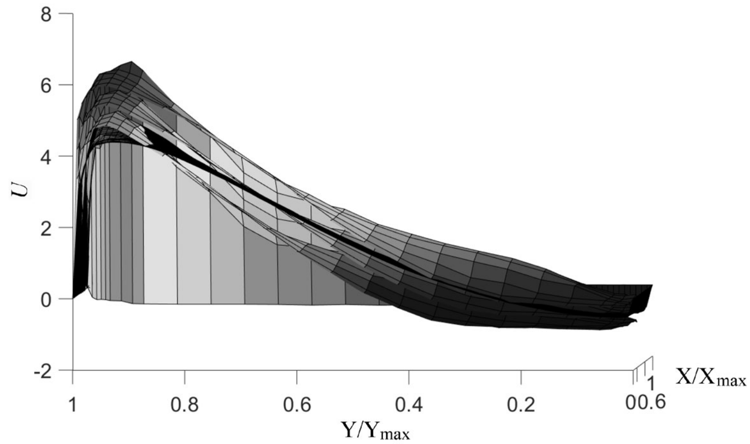

Fig. 10. Comparison of results of experiment, measurement, and modeling for cross section 3. Experimental surfaces of axial velocity component, which reflect limits of measurement errors, are shown, as well as surface of axial velocity component obtained from calculations using k-ε turbulence model.

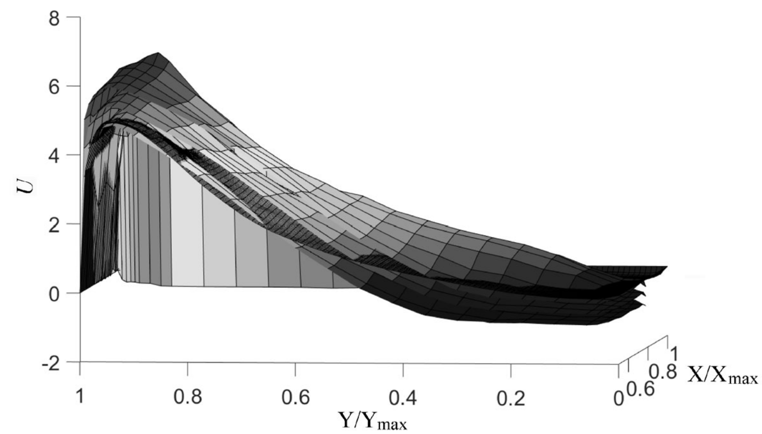

Fig. 11. Comparison of results of experiment, measurement, and modeling for cross section 3. Experimental surfaces of axial velocity component, which reflect limits of measurement errors, are shown, as well as surface of axial velocity component obtained from calculations using Reynolds stress transfer model.

REFERENCES

1. Balzhinimaev, B.S., Ivanov, S.Yu., Kabardin, I.K., Ezendeeva, D.P., Gordienko, M.R., Kakaulin, S.V., Klimonov, I.A., Sycheva, T.I., Usov, E.V., and Yavorsky, N.I., Computational Analysis of Gas Flow in Gas Distributor Breadboard for Creating Efficient Devices to Remove Volatile Organic Compounds, *J. Eng. Therm.*, 2019, vol. 28, no. 3, pp. 372–380.
2. Kabardin, I.K., Klimonov, I.A., Usov, E.V., Yavorsky, N.I., Kabardin, A.K., Kakaulin, S.V., Ezendeeva, D.P., Gordienko, M.R., Polyakova, V.I., and Pravdina, M.H., Calculation-Experiment Study of Gas Motion in Controlled Turning-and-Diverging Flow, *J. Eng. Therm.*, 2020, vol. 29, no. 3, pp. 1–9.
3. Launder, B.E. and Spalding, D.B., The Numerical Computation of Turbulent Flows, *Comp. Meth. Appl. Mech. Engin.*, 1974, vol. 3, pp. 269–289.
4. Andersson, B., Andersson, R., Häkansson, L., Mortensen, M., Sudiyo, L., Wachem, B., and Hellström, L., *Computational Fluid Dynamics for Engineers*, Cambridge University Press, 2012.